

Complex Filters Applied to Fingerprint Images Detecting Prominent Symmetry Points Used for Alignment

Kenneth Nilsson and Josef Bigun

School of Information Science, Computer and Electrical Engineering (IDE)
Halmstad University, P.O. Box 823, SE-301 18 Halmstad, Sweden.
`Kenneth.Nilsson@ide.hh.se`, `Josef.Bigun@ide.hh.se`

Abstract. For the alignment of two fingerprints position of certain landmarks are needed. These should be automatically extracted with low misidentification rate. As landmarks we suggest the prominent symmetry points (core-points) in the fingerprint. They are extracted from the complex orientation field estimated from the global structure of the fingerprint, i.e. the overall pattern of the ridges and valleys. Complex filters, applied to the orientation field in multiple resolution scales, are used to detect the symmetry and the type of symmetry. Experimental results are reported.

1 Introduction

A fingerprint image can be said to have two structures, the global structure and the local structure. By the global structure we mean the overall pattern of the ridges and valleys, and the local structure the detailed patterns around a minutiae point (a position in the fingerprint where a ridge is suddenly broken or two ridges are merged).

Direct use of the local structure in the identification/verification process is sensitive to noise, i.e. poor performance for low quality fingerprints can be foreseen. Compared to the local structure the global structure is very stable even when the fingerprint is of poor quality [1].

Here we suggest to first align the reference and the test fingerprint before using the local structure for the identification/verification. In the alignment step the global structure of the fingerprint is used. When the two fingerprints are aligned (registered) we can match "point-by-point" the local structure for selected positions more robustly than directly extracting them and then performing a matching of minutiae. The reference fingerprint is assumed to have a better quality than the test image. The rationale behind this is that the test image is captured under less controlled conditions than the reference image. For the alignment we need the positions of certain landmarks (core-points) in the fingerprint that are less prone to misidentification in automatic recognition. Typical core-points (arch and delta type) are shown in Fig. 1. As can be seen these points have special symmetry properties which make them easy to identify by humans.

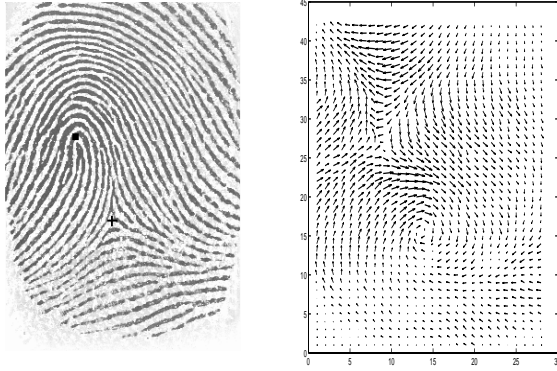


Fig. 1. Left: marked core-points. Right: orientation field as double of the gradient direction

We suggest to use complex filters to detect the symmetry and the type of symmetry. Two different filters are used, one for the "arch-type" core-point and one for the "delta-type" core-point. The filtering is applied to complex images, i.e. the orientation tensor field [2] in different scales. The orientation tensor field is often used to represent the global structure in a fingerprint [1, 3]. Also when estimating curvature in oriented patterns the orientation field is used [4, 5]. An original fingerprint and its estimated orientation field are shown in Fig. 1 as illustration.

This paper presents the theory and experimental results for automatic extraction of core-points from the global structure using complex filters designed to detect prominent symmetries.

2 Symmetry Point Extraction

2.1 Filters for Rotational Symmetry Detection

Complex filters, of order n , for the detection of patterns with radial symmetries are modelled by $\exp\{in\varphi\}$ [6, 7, 8]. An approximation of these filters in gaussian windows yields $(x + iy)^n g(x, y)$ where g is a gaussian [9].

It is worth to note that these filters are not applied to the original fingerprint image but instead they are applied to the complex valued tensor orientation field image $z(x, y) = (f_x + if_y)^2$. Here f_x is the derivative of the original image in the x -direction and f_y is the derivative in the y -direction.

In our experiments we use filters of the first order symmetry, i.e.

$$h_1(x, y) = r \exp\{i\varphi\} g(x, y) \approx (x + iy)g(x, y) \text{ and}$$

$$h_2 = r \exp\{-i\varphi\} g(x, y) \approx (x - iy)g(x, y)$$

although extension to second and higher orders symmetries is straightforward. Fig. 2 shows the complex filter h_1 and h_2 respectively. h_1 detects symmetry of "arch-type" and h_2 of "delta-type".

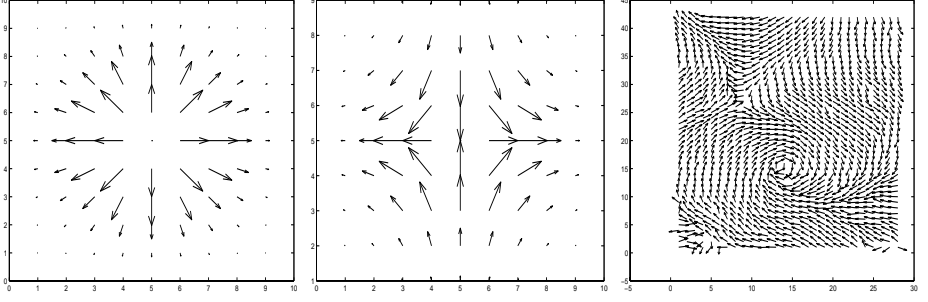


Fig. 2. Left: the complex filter h_1 . Middle: the complex filter h_2 . Right: the complex orientation field (magnitude=1) for the image in Fig. 1.

The filter response is $\mu \exp\{i\alpha\}$, where μ is a certainty measure of symmetry, and α is the "member" of that symmetry family, here the geometric orientation of the symmetric pattern.

2.2 Multi-scale Filtering

The complex orientation field $z(x, y)$ is represented by a four level gaussian pyramid. Level 3 has the lowest, and level 0 has the highest resolution. We only use the angle of the complex orientation field, i.e. the magnitude is set to one in $z(x, y)$ in multiscale filtering. The arch and delta filtering is applied on each resolution. The complex filter response is called c_{nk} , where $k=3, 2, 1$ and 0 are the resolution levels, and $n=1, 2$ are the filter types (arch and delta).

Fig. 2 (right) shows the orientation field, level 3, with magnitude set to one for the original image in Fig. 1. Fig. 3 shows the magnitude of the filter responses of filter h_1 (called μ_{1k}), and h_2 (called μ_{2k}) for levels $k=3, 2$, and 1 . The filters are applied to the image in Fig. 1.

2.3 Maximum Filter Response

In order to improve the selectivity of the filters, i.e. a filter should give a strong response only to one of the symmetries (here: h_1 to "arch-type" symmetry and h_2 to "delta-type" symmetry) we use the following rules to sharpen the magnitude of the filter responses [10]:

$$\begin{cases} s_{1k} = \mu_{1k}(1 - \mu_{2k}) \\ s_{2k} = \mu_{2k}(1 - \mu_{1k}) \end{cases} \quad (1)$$

with (levels) $k=0, 1, 2$, and 3 . Fig. 4 shows the responses s_{1k} , and s_{2k} .

The complex filter response is $s_k \exp\{i\alpha_{nk}\}$, where s_k is a measure of certainty for that there is a symmetry of type n at resolution k , and α_{nk} tells how much the symmetric pattern is rotated compared to a fixed reference.

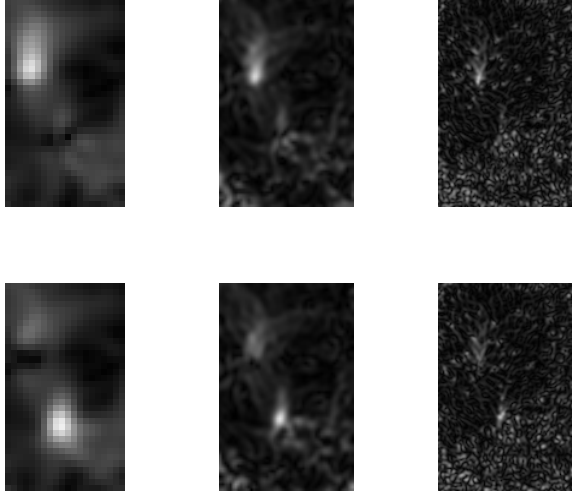


Fig. 3. Row1: filter response μ_{1k} , $k=3,2,1$. Row2: filter response μ_{2k} , $k=3,2,1$.

To find the position of a possible core-point in a fingerprint the maximum filter response is extracted in image s_{13} and in s_{23} (level 3). To get even further precision in maximum localization a new search is done in lower levels of the pyramid i.e. in s_{n2} , s_{n1} , and s_{n0} for both $n=1, 2$. The search is done in a window computed in the previous higher level (lower resolution).

At a resolution (level k), if $s_{nk}(x_j, y_j)$ is higher than a threshold a core-point is found and its position (x_j, y_j) and the complex filter response $c_{nk}(x_j, y_j)$ are noted.

3 Implementation

The 2D scalar product $\langle h, z \rangle$ is calculated for each image point, where $h = (x + iy)^n g(x, y)$ is the complex filter of order n , and z is the complex orientation field, i.e. this is a 2D complex convolution between the image z and the filter h . Due to the separable property of a 2D gaussian function, the filter h can be written as: $h = (x + iy)^n g(x)g(y)$.

The 2D convolution can therefore be computed by using several 1D convolutions. A faster implementation can then be achieved.

This is now shown in detail only for a first and second order filter. The second order filter is shown only for reference purposes for other applications than fingerprints. First order filter:

$$h = (x + iy)g(x)g(y) = xg(x)g(y) + i[yg(y)g(x)].$$

Second order filter:

$$\begin{aligned} h &= (x + iy)^2 g(x)g(y) = (x^2 - y^2 + i2xy)g(x)g(y) \\ &= x^2 g(x)g(y) - y^2 g(y)g(x) + i2[xg(x)yg(y)]. \end{aligned}$$

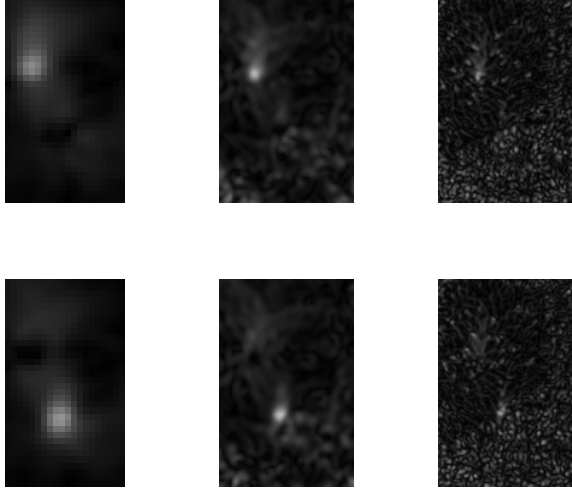


Fig. 4. Row1: filter response s_{1k} , $k=3,2,1$. Row2: filter response s_{2k} , $k=3,2,1$.

By designing the 1D filter $g(t)$, $tg(t)$, and $t^2g(t)$ the filtering of the image z can be done as:

$g(y) * ((xg(x))^t * z(x, y)) + ig(x)^t * ((yg(y)) * z(x, y))$ for first order filters and $g(y) * ((x^2g(x))^t * z(x, y)) - g(x)^t * ((y^2g(y)) * z(x, y)) + i2[(yg(y)) * ((xg(x))^t * z(x, y))]$ for the second order filters. The symbol $*$ represents the convolution operation.

Also in computing the orientation field z , 1D convolutions are used instead of a 2D convolution. This is possible as the derivative filters used are the first partial derivatives of a 2D gaussian function and therefore separable. For further details on derivatives of gaussian in complex fields we refer to [9].

4 Experiments

The FVC2000 fingerprint database, DB2 set A is used in the experiments. A total of 800 fingerprints (100 persons, 8 fingerprint/person) are captured using a low cost capacitive sensor. The size of an image is 364 x 256 pixels, and the resolution is 500 dpi. It is worth to note that FVC2000 is constructed for the purpose of grading the performance of fingerprint recognition systems, and contains many poor quality fingerprints.

Only filters of the first order ($n=1$, and $n=-1$) have been used in this work, as these two filters were capable to detect the different types of core-points that could be found in fingerprints of FVC2000.

The orientation tensor field $z(x, y) = (f_x + if_y)^2$ has been computed by using a $\sigma = 0.8$. A small value on σ is chosen because we wanted to capture fine details in the fingerprint. We represent the orientation field z using a gaussian pyramid

in four levels. Level 3 has the lowest resolution 42×28 , level 2: 87×60 , level 1: 178×124 , and level 0: 360×252 . A $\sigma = 0.8$ is used in the smoothing before downsampling by 2. In level 3 we have a smooth orientation field that capture the global structure in the fingerprint.

Complex filtering for symmetry detection is done in each level by using 1D filters (g , tg , t^2g with $\sigma = 1.5$) in x and y directions as explained in Section 3.

For level 3 only, we compute a modified complex filter response. This is done in two steps. Firstly, we locally downweight c_{n3} if a point has low orientation certainty via $c_{n3} \cdot (g_1 * |z_3|)$ where g_1 is a gaussian function with $\sigma = 1.5$ and $*$ is pointwise multiplication. This step downweights the low certainty orientation areas of the image. Secondly, we pointwise multiply a large gaussian which is 1 at the centre and decreases significantly towards the border via $c_{n3} \cdot g_2$ with g_2 having standard deviations as one third of the height of c_{n3} ($=11.7$) and one third of the width of c_{n3} ($=7.0$). This step downweights the border regions of the fingerprint image. Next these two complex images are averaged according to:

$$c_{n3} \leftarrow 0.5(c_{n3} \cdot (g_1 * |z_3|) + c_{n3} \cdot g_2) \quad (2)$$

so that points with high quality orientation close to the image border (and elsewhere) are not suppressed while border points are generally suppressed due to the low image quality induced by low mechanical pressure at the fingerprint frontiers. The result is reassigned to c_{n3} .

After the modification the c_{n3} image is processed further to sharpen the selectivity according to Eq. 1. This yields the image s_{n3} and the maximum in s_{13} and s_{23} image are found.

A window size of 13×13 is used when searching for the maximum responses in the next lower resolution s_{12} and s_{22} . A point is accepted as a core-point if a filter response s_{n2} has a value higher than a threshold, i.e. an acceptance of a core-point is done on level 2. To improve the precision in position of the accepted core-point the window procedure is applied to resolution level 1.

Due to the fact that the true position of the core-points in the fingerprint are not known, we were obliged to do a visual inspection of the positions of the estimated core-points for each fingerprint in the database. A total of 800 fingerprints are inspected. In each fingerprint the position of the maximal filter response in level 2 for each type of core-point (arch, delta) has been noted. Here arched type is marked with a square, and a delta type with a cross. Also, the certainty measure s_{n2} for the maximal filter response of the two types is printed out.

Fig. 5 shows examples of images in the visual inspection. For the image on the left the certainty s_{12} at the marked arch position was 0.64 whereas for the delta point s_{22} was 0.61 (1 represents max certainty). The corresponding figures for the estimated max points in the middle image were 0.70 and 0.66 and for the right image 0.60 and 0.30.

If the certainty measure is higher than a threshold T the point is classified as a core-point. If the position is incorrect despite that the certainty is high the point is classified as "False core-point". This case is a false acceptance case (FA).



Fig. 5. Fingerprints in the visual inspection

Table 1. Results of recognition

FVC2000 database. (800 fingerprints)	Arch- type	Arch- type	Delta- type	Delta- type
	No.	%	No.	%
False core-point (FA)	41	5.1	18	2.3
False not core-point (FR)	46	5.8	23	2.9

If the certainty measure is lower than a threshold T the point is classified as being not a core-point. If the point is despite that a core-point and its position is correct, the point is classified as a "False not core-point". This is in other words a false rejection of a core-point (FR).

The classification of arch type core-points is done by using a threshold value of $T = 0.45$ and in the classification of delta type core-points $T = 0.5$ is used. This choice was made to reach approximately Equal Error Rate (EER). The overall result is presented in Table 1.

We are not aware of other researchers who have attempted to quantify recognition of global core-points. For this reason it has not been possible for us to provide comparative results in this paper.

5 Conclusion

Given the difficulty level of the used database the results reported in this paper are, we think, very encouraging for implementing an automatic fingerprint verification scheme.

The relative high number of misclassification of arch type core-points can be tracked to the same global structure of a fingerprint, namely plain arch (FBI's



Fig. 6. Left: "False not core-points". Right: "False core-point, cross".

classification scheme [1]). For this failing structure both filters give strong responses, and therefore low certainty measures when using the selectivity rule (Eq. 1). Also, there is a spatially spread out of strong filter responses compared to the arch structure which gives an uncertainty in the position. This is expected to be improved in future research by including higher orders symmetries, as well as alternative selection rules. A border problem also exist, i.e. the border between the background and the fingerprint gives high values in the orientation field image and therefore "False core-points".

Fig. 6 shows examples of "False not core-point" to the left: with its certainty measures $s_{12} = 0.40$ $s_{22} = 0.40$, and to the right: "False core-point" with its certainty measures $s_{12} = 0.65$ $s_{22} = 0.60$. In the experiment we only use one certainty measure (maximal filter response from one of the filters) to classify the point being a core-point or not. Instead we could represent each point by its feature vector, where the features are the responses from the two filters. The feature vector can then be used to classify each point as a core-point or not, and also which type of core-point it is.

Acknowledgment

This work has been possible by support from the Swedish national SSF-program VISIT.

References

- [1] R. Capelli, A. Lumini, D. Maio, and D. Maltoni. Fingerprint classification by directional image partitioning. *IEEE Transactions on Pattern Analysis and Machine Intelligence*, 21(5):402–421, May 1999.
- [2] J. Bigun and G. H. Granlund. Optimal orientation detection of linear symmetry. *IEEE Computer Society Press, Washington, DC*, pages 433–438, June 1987. In First International Conference on Computer Vision, ICCV (London).

- [3] A. K. Jain, S. Prabhakar, L. Hong, and S. Pankanti. Filterbank-based fingerprint matching. *IEEE Transactions on Image Processing*, 9(5):846–859, May 2000.
- [4] J. Van de Weijer, L. J. van Vliet, P. W. Verbeek, and M. van Ginkel. Curvature estimation in oriented patterns using curvilinear models applied to gradient vector fields. *IEEE Transactions on Pattern Analysis and Machine Intelligence*, 23(9):1035–1042, September 2001.
- [5] M. K. Koo and A. Kot. *Curvature-based singular points detection*. Springer LNCS 2091, Bigun and Smeraldi Eds. Springer, 2001. Third International Conference AVBPA 2001, Halmstad, Sweden.
- [6] J. Bigun. Recognition of local symmetries in gray value images by harmonic functions. *Ninth International Conference on Pattern Recognition, Rome*, pages 345–347, 1988.
- [7] H. Knutsson, M. Hedlund, and G. H. Granlund. Apparatus for determining the degree of consistency of a feature in a region of an image that is divided into discrete picture elements. *US. Patent, 4,747,152*, 1988.
- [8] J. Bigun. Pattern recognition in images by symmetries and coordinate transformations. *Computer Vision and Image Understanding*, 68(3):290–307, December 1997.
- [9] J. Bigun and T. Bigun. Symmetry derivatives of gaussians illustrated by cross tracking. *Research report IDE-0131*, September 2001.
- [10] B. Johansson. *Multiscale curvature detection in computer vision*. Tech. lic., Linköping University, Linköping University, Dep. Electrical Eng., SE-581 83, 2001.